# Evaluation of Residual Stresses in Heat Treated AISI 5115 and AISI 52100 Steels via Analysis of Instrumented Sharp Indentation Load-Unload Cycle

Osman Culha
Dokuz Eylul University, Faculty of Engineering
Department of Metallurgical and Materials Engineering, Turkey
osman.culha@deu.edu.tr

Seher Tas
Dokuz Eylul University, Faculty of Engineering
Department of Metallurgical and Materials Engineering, Turkey
seher.tas@ogr.deu.edu.tr

Mustafa Toparli
Dokuz Eylul University, Faculty of Engineering
Department of Metallurgical and Materials Engineering, Turkey
mustafa.toparli@deu.edu.tr

**Abstract:** In this research, heat treated AISI 5115 (16MnCr5) cementation and AISI 52100 roller bearing steels were investigated. The specimens that were prepared before and after heat treatment application were sectioned via wire-erosion machine. Specimens were properly sanded and polished to get a smooth surface. Optical micrographs of each specimen were taken by a Nikon Eclipse ME 600 metallographic microscope. These specimens were then examined by using a Dynamic Ultra Micro Hardness (DUH) tester under a set of maximum loads of 200, 400, 600, 800, and 1000 mN. For each heat treated and non-heat treated specimen subjected to load-unload cycle under the same amount of maximum load, load vs. penetration depth curves were plotted. By comparing the resultant load-unload curves, types of the residual stresses were determined. Individual calculations were made for tensile and compressive residual stresses to obtain the residual stress values.

## Introduction

Residual Stress after various product stages such as welding, casting, surface processing and heat treatment process that remain in parts. Varieties relevant with welding manufacturing, casting, surface treatments and heat treatment effect mainly reason become residual stress. Residual stress because of in part after manufacturing will be applied external stress during service, effect with residual stress (Dilmeç et al., 2008). In this case, contained residual stress in a part, real applied condition may be much different from estimated that results obtained by analysis/calculate on part. Tensile and compressive residual stresses consist of thermal stress resulting from cooling difference between surface and core of material. This stresses may be beneficial or harmful to the material performance (Asi & Asi, 2003). While, tensile stresses decrease fatigue life of material so early damage, compressive stresses act to increase fatigue life of materials. Successful heat treatment process may hinge upon achieving not only the appropriate surface finish, hardness, but also a residual stress distribution producing the longest component life

During surface hardened process such as cementation and nitruration, surfaces are heated in carbon or nitrogen atmosphere. These of result, volume of surfaces grow up and compressive residual stresses are becoming in the surfaces. Depending on rising hardened layer thickness in the cemented steel increase compressive residual stresses. Therefore abrasion resistance and fatigue strength in parts of surfaces is increased (Karataş et al., 2001). To understand the significance of these effects on the production of parts such as bearing ball and gears, and to evaluate material's performance during service need to know level of residual stress.

There are many destructive and nondestructive methods in order to measure the residual stresses in materials. Non-destructive residual stress measurement techniques make use of different characteristics of samples in order to obtain residual stress. There are magnetic method, ultrasonic method, raman spectroscopy, X-ray diffraction and neutron diffraction. The main principle of the destructive methods is that by removing some part of the sample depending on the technique. Sahin et al. (2003) determined residual stresses near the surface of the material by the hole-drilling strain-gage method. In addition, the contour method is one of the

recent destructive residual stress measurement techniques. Turski and Edwards (2009) examined the measurement of transverse residual stresses within the bead-on-plate weld specimen using the contour method. Suresh and Giannakopoulos (1998) have first introduced indentation technique which is a destructive technique for estimating residual stress. Comparing with traditional techniques, the depth-sensing indentation technique provides a quick and effective method of measuring the residual stress field (Chen et al., 2006). In this technique, experimentally determined the type and magnitude of residual stresses from automatically drawn load-unload curves from computer which connected microhardness test equipment, can be easily calculated residual stress. Being a destructive testing method, instrumented sharp indentation has been applied in recent years as a technique to evaluate the inhomogeneously distributed residual stresses caused by plastic deformation or thermal effects in welded, cast, surface processed and heat treated materials. By utilizing instrumented sharp indentation, residual stresses produced by various different processes on material surfaces can be directly measured. It's evident through current studies that results obtained by using this technique are robust enough to compare with other methods. As a fast and reliable means of residual stress evaluation, it's believed that this technique will become a common practice in the foreseeable future.

In the present study, subjected to heat treatment of AISI 5115 (16MnCr5) and AISI 52100 (100Cr6) steels were measured in the bottom of surface the residual stresses using indentation techniques.

## Instrumented Indentation Method

The microindentation technique (Nishibori et al., 1978; Dub et al., 2002) has been developed in some decades, and the mechanical properties within a sub-micron or nano scale are widely discussed. The techniques are expected to be useful for measurement of the mechanical properties of thin films or local structure of various materials. While employing the instrumented indentation technique at nanoscale one can directly determine the nanohardness, Young's modulus and the deformation characteristics (Reibold et al., 2005). From the loading and unloading curve the nature of elastic–plastic transition can be analyzed.

Elastic modulus $E$ and microhardness $H$ can be obtained with the load and penetration depth data (Uzun et al. 2005). During indenter loading, test material is subjected to both elastic and plastic deformation. The three key parameters needed to determine the hardness and modulus are the peak load ($P_{max}$), the contact area ($A_c$) and the initial unloading contact stiffness ($S$). Similar to the conventional microhardness testing, the micro indentation hardness is usually defined as the ratio of the peak indentation load, $P_{max}$, to the projected area of the hardness impression, $A$c, i.e.

$$H = \frac{P_{\max}}{A_c} = \frac{P_{\max}}{26.43 h_c^{\,2}} \qquad (A_c = 26.43 h_c^{\,2}) \tag{1}$$

Different approaches for deducing the contact depth, $h$c, from the resultant load displacement curve have been purposed and perhaps the most widely used one is that of Oliver and Pharr (Oliver &.Pharr, 1992). The Oliver and Pharr (1992) data analysis procedure begins by fitting unloading curve to an empirical power-law relation.

$$P = \alpha(h - h_f)^m \tag{2}$$

where $P$ is the indentation load, $h$ is the penetration depth, $h_f$ is the final unloading depth and $\alpha$ and $m$ are empirically determined fitting parameters. Using the initial part of the unloading curve, both stiffness and contact depth are determined by differentiating Eq. (2) at the maximum depth of penetration, $h = h_{max}$. Then, the stiffness of the contact is given by

$$S = \frac{dP}{dh} = \frac{2}{\sqrt{\pi}} E_r \sqrt{A_c} \tag{3}$$

Where $E_r$ is the reduced elastic modulus.

In this study, the Oliver and Pharr (1992) method was used to calculate the initial stiffness ($S$), contact depth ($h_c$) and hence reduced modulus ($E_r$) and hardness (HV).

$$\frac{1}{E_r} = \frac{1-\nu^2}{E} + \frac{1-\nu_0^{\,2}}{E_o} \tag{4}$$

Where E and ν are Young's modulus and Poisson's ratio for the specimen, and $E_o$ and $\nu_o$ are the same parameter for the indenter.

As explained above, instrumented indentation is characterized by a sharp rigid indenter which mechanical properties are known (frequently made of a very hard material like diamond) penetrating normally into a homogeneous solid where the indentation load, P, and displacement, h, are continuously recorded during one complete cycle of loading and unloading (Figure 1).

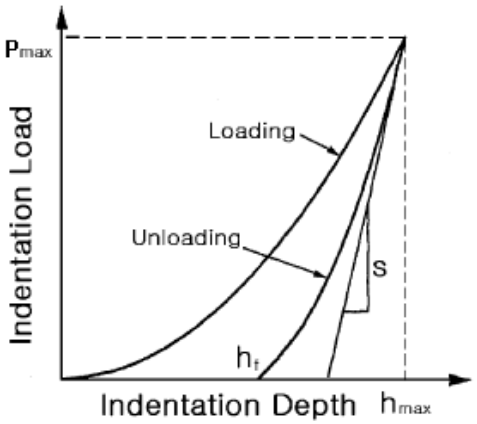


**Figure 1:** Schematic graph of the indentation load–depth curve (Son et al., 2003)

Measured residual stress is based on the calculation of the difference between the indentation contact areas of with and without stressed surfaces by analyzing ‘‘indentation load–depth’’ data according to the below equations (Suresh & Giannakopoulos, 1998):

For tensile residual stress

$$A_c/A_o = (1-(\sigma_r / \rho ave))^{-1} \quad (5a)$$

For compressive residual stress

$$A_c/A_o = (1+(\sigma_r \sin\alpha / \rho ave))^{-1} \quad (5b)$$

where $A_c$ and $A_o$ are the indentation contact areas with and without residual stress ($\sigma_r$), respectively. $\alpha$ is a geometric factor, where a is related to the indentation angle of the indenter. If the Vickers pyramid indenter is used $\alpha = 22^o$. $\rho_{ave}$ is the average contact pressure, $\rho_{ave} = P_{max}/A_{max}$

Depend on the type of residual stress (tensile or compressive) as shown in Figure 2 if the indentation contact area ratio ($A_c/A_o$) is known then $\sigma_r$ values can be calculated simply from Equation (1a) or (1b).

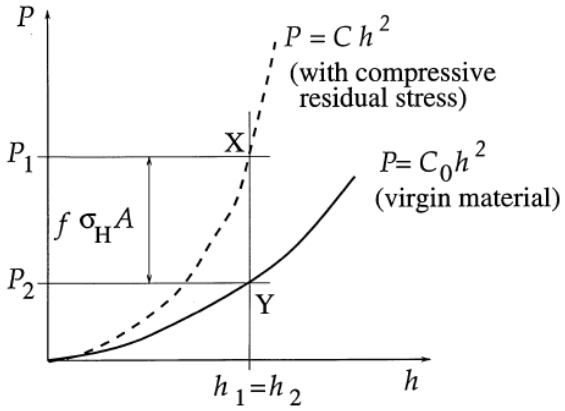


**Figure 2:** The indentation load-depth (P-h) curves for the surfaces with and without residual stresses.

We now seek to derive the effects of a compressive residual stress on the contact areas and indentation penetration depths. Figure 2 schematically shows the load-depth curve for the indentation of the virgin material, and that for the substrate with an equibiaxial compressive residual stress. Assume that the following loading history takes place. The material with the residual stress is first indented with a load $P_1$ which causes the indenter to penetrate it by a depth $h_1$. This point is denoted by the symbol X in Figure 2 (Suresh & Giannakopoulos, 1998)

Keeping the indentation depth $h_1$ constant, let the indented material now undergo a complete relaxation of the residual stress, i.e. let the residual stress relax from $\sigma_{xR}{}^o = \sigma_{yR}{}^o$ 0 to zero at a fixed penetration depth, $h_1=h_2$. In order for the average contact pressure pave to remain invariant, the equivalent plastic strain beneath the indenter should be preserved, as noted earlier. Consequently, the change in the stress state of the material beneath the indenter during the release of this compressive residual stress must be hydrostatic. The resulting

tensile hydrostatic stress, $\sigma_H$, $\sigma_{xR}^o$, $\sigma_{yR}^o$, $\sigma_{zR}^o$ can be regarded as introducing an effective differential force of magnitude $\sigma_H fA$ in the z direction, i.e. in the direction of the applied indentation load, as shown in Figure 3, where f= sinα. Thus, as the compressive residual stress, $\sigma_{xR}^o$, $\sigma_{yR}^o$ is released and the point of indentation moves from location X to location Y in the P-h curves in Figure 2, the contact force effectively decreases from $P_1$ to $P_2$ at a constant penetration depth, $h_1=h_2$. In summary, for a fixed indenter penetration depth and for X-Y in Figure 2,

$$P_1-P_2= \sigma_H fA=- \sigma_{xR}^o fA= -\sigma_{yR}^o fA$$

From the equation (2) can be obtained ratio ($A_c/A_o$) :

$$\frac{A}{Ao}=\left(1+\frac{\sigma_y{}^R}{\sigma_u}\right)^{-1}.\left(1+\frac{\sigma_y}{\sigma_u}\right).\left(1+\ln\frac{E\tan\alpha}{3\sigma_y{}^R}\right)^{-1}.\left(1+\ln\frac{E\tan\alpha}{3\sigma_y}\right) \tag{6}$$

where $\sigma_y$ and $\sigma_y^R$ are the yield strengths of the surface with and without residual stress, respectively, $\sigma_u$ is the ultimate strength (Suresh & Giannakopoulos, 1998).

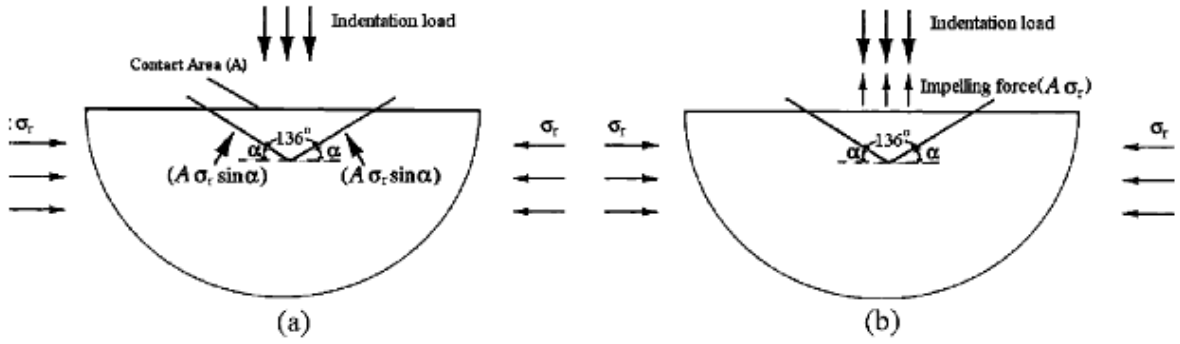


**Figure 3:** Schematic representation of residual stress while indenter is under contact position with material a) for Suresh and Giannakopoulos (1998) b) for Atar et al. (2003)

Suresh and Giannakopoulos (1998) reported that according to the upper-bound solution of the compressive residual stress, the magnitude of the force acting normal to the inclined faces of the indenter during indentation is $\sigma_r fA$ as shown in Figure 3a. Since $\alpha=22^o$ for the Vickers pyramid indenter, the geometric factor f =sinα is noted as 0.375 theoretically. In the present study, the geometric factor was calculated experimentally as 1, which corresponds to an a value of $90^o$. This indicates that the impelling force having a value of $\sigma_r A$ is acting against the applied indentation load in the direction of indentation (perpendicular to the indentation contact area) rather than the component of the residual stress acting normal to the inclined faces of the indenter. Thus, Net indentation load =applied indentation load- impelling force as shown in Figure 3b. Therefore, for the calculation of the residual compressive stress in materials by utilizing the Vickers pyramid indenter, Eq. (5b) should be modified as (Atar et al., 2003):

$$\frac{A}{A_o}=\left\{1+\left(\frac{\sigma_r}{\rho_{ave}}\right)\right\}^{-1} \tag{7}$$

In this study, we draw attention to residual stress calculation of AISI 5115 and 52100 bulk material after heat treated by indentation method. In this context, Both Atar et al. (2003) and Suresh & Giannakopoulos (1998) method were used and compare with each other. Firstly, mechanical properties of materials were examined by Shimadzu Dynamic Ultra-micro hardness test machine for estimating Young's modulus due to load-unload sensing analysis, in addition to mechanical investigation hardness-force and Young's modulus-force curves of the coatings were obtained. Load depended elastic modulus and hardness were obtained at 200 mN, 4000 mN, 600 mN, 800 mN and 1000 mN applied peak loads. After obtaining characteristics indentation curves under applied loads of different quality virgin and heat treated materials, residual stresses were calculated with two different indentation approaches.

## Experimental Study

High carbon through-hardening steel AISI 52100 and case-carburized low carbon steel AISI 5115 are used for antifriction bearings and gears, shafts, axles, cam. (Stickels & Janotik, 1980). Case-carburized parts and

cemented steels develop compressive residual stresses at the surface. Compressive residual stresses at the surface are beneficial performance of material, which during service.

In this experimental study, samples were manufactured from rods of an AISI E52100 ball bearing steel and AISI 5115 (16MnCr5) carburizing steel. This samples chemical composition is given in Table 1 and Table 2. The samples turned a disk with a thickness of 0.50mm and a diameter of Ø22mm after the samples were cut from rod at a wire EDM machines samples to measure with and without the stresses before and after heat treatment processing, respectively.

| C (%) | Si(%) | Mn(%) | P(%) | S(%) | Cr(%) | Ni(%) | Cu(%) |
|---|---|---|---|---|---|---|---|
| 0.966 | 0.236 | 0.468 | 0.008 | 0.005 | 1.580 | 0.107 | 0.110 |

**Table 1:** Chemical composition of the AISI 52100(100Cr6) ball bearing steel

| C (%) | Si (%) | Mn(%) | P(%) | S(%) | Cr(%) |
|---|---|---|---|---|---|
| 0.14-0.16 | 0.15-0.40 | 1.0-1.30 | 0.035 | 0.05 | 0.8-1.1 |

**Table 2:** Chemical composition of the AISI 5115 (16MnCr5) carburized steel

Carburizing programs were carried out in gas atmosphere at 960°C and 840°C for16MnCr5 and 100Cr6, respectively at heat treatment. During the carburizing process the carbon potential of batch furnaces was adjusted to 1.2 % C and 0.45 % C at 960°C and 840°C and then reduced to maintain the final surface carbon content of the 16MnCr5 specimen below 0.8% C and but increased above 0.8% C of the final surface carbon content for 100Cr6 specimen. Specimens were processed in the direct quenched condition and then were tempered at 80°C for 20-30 minutes. Surface preparation of the disks was done by grinding and polished.

These specimens were then examined by using a Dynamic Ultra Micro Hardness (DUH) tester under a set of maximum loads of 200, 400, 600, 800, and 1000 mN. For each heat treated and non-heat treated specimen subjected to load-unload cycle under the same amount of maximum load, load vs. penetration depth curves were plotted. During the test load-depth (P-h), elasticity modulus and hardness data of each samples were recorded with connected computer. By comparing the resultant load-unload curves, types of the residual stresses were determined. Individual calculations were made for tensile and compressive residual stresses to obtain the residual stress values.

## Results and Discussion

The mechanical properties such as hardness, Young's modulus, fracture toughness, ductility, etc are important parameters for industrial application. Shimadzu Dynamic Ultra Micro Hardness Testing machine is used for determination hardness variation and young modulus of FeB layers. Different loads such as 200, 400, 600, 800, 1000 mN are applied for determination of hardness and Young's modulus. Loading and unloading curves of AISI 5115 and 52100 before and after heat treated materials are shown in Figure 4 and 5. According to the results, compressive characteristics residual stresses were obtained for each material.

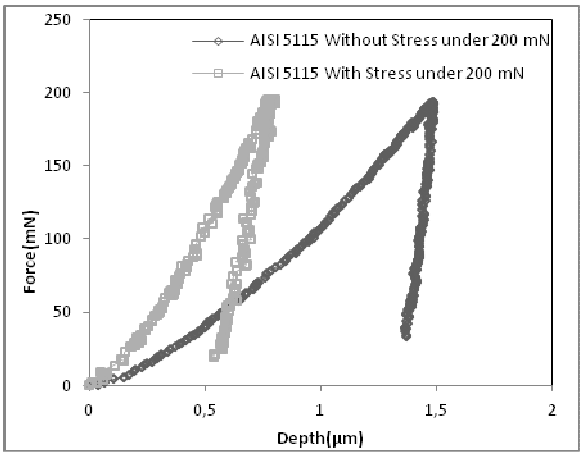


1.

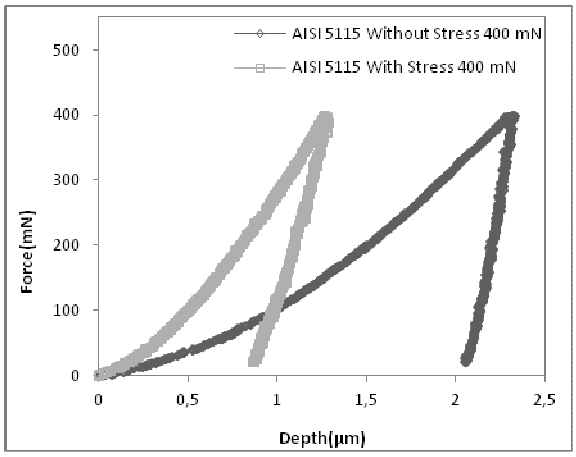


(b)

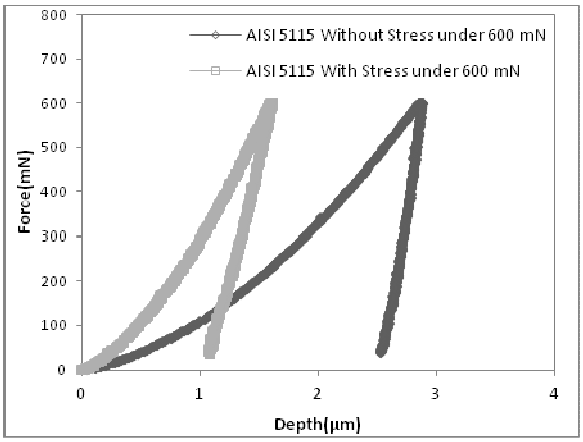


(c)

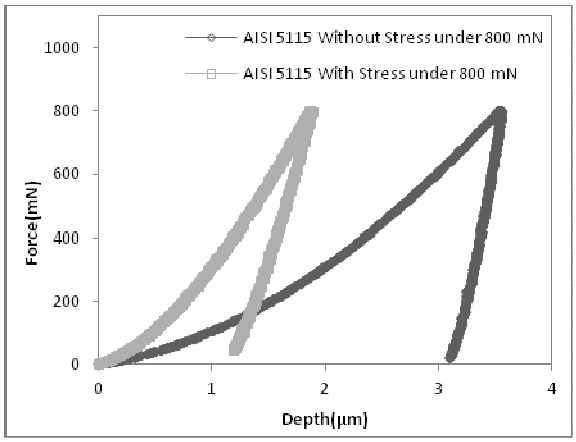


(d)

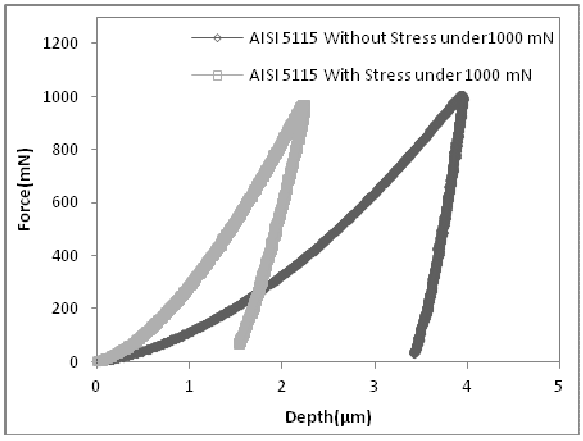


(e)

**Figure 4:** Loading- unloading curves of AISI 5115 quality steels under a**)** 200 mN **b)** 400 mN **c)** 600 mN **d)** 800 mN **e)** 1000mN

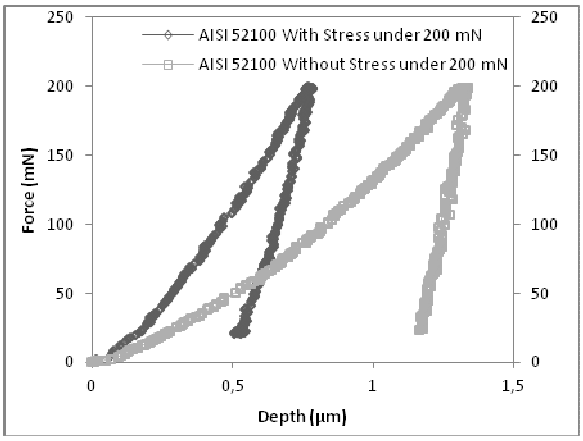


(a)

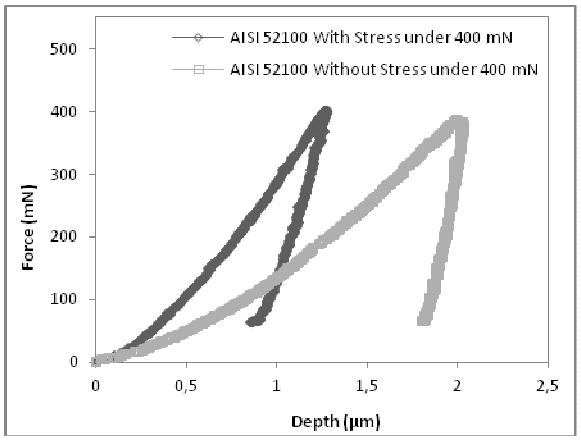


(b)

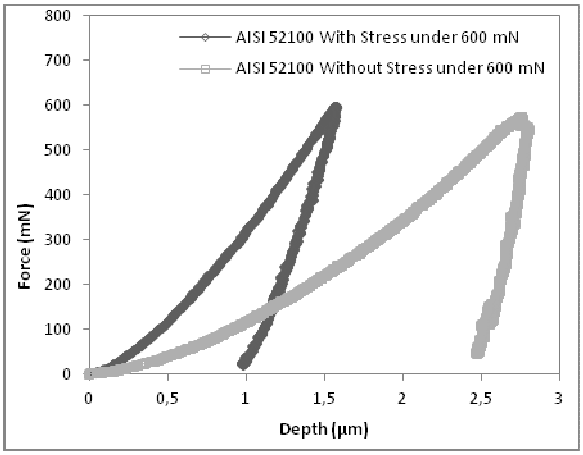


(c)

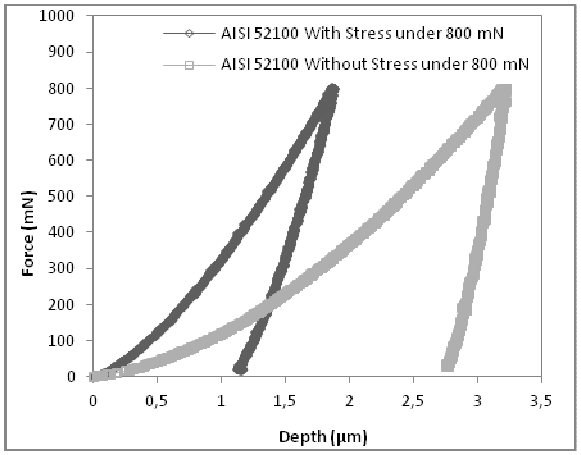


(d)

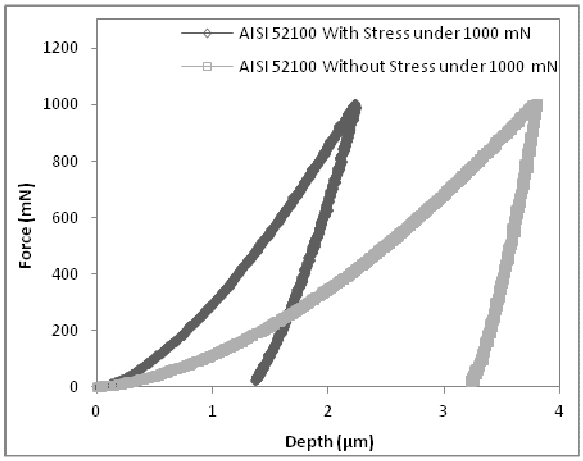


(e)

**Figure 5:** Loading- unloading curves of AISI 52100 quality steels under a**)** 200 mN **b)** 400 mN **c)** 600 mN **d)** 800 mN **e)** 1000mN

The calculated Young's modulus of AISI5115 and AISI52100 quality steels with and without stress under different applied peak loads are shown in Figure 6. According to the results, Young's moduli of stressed and unstressed materials are decreased with increasing applied loads.

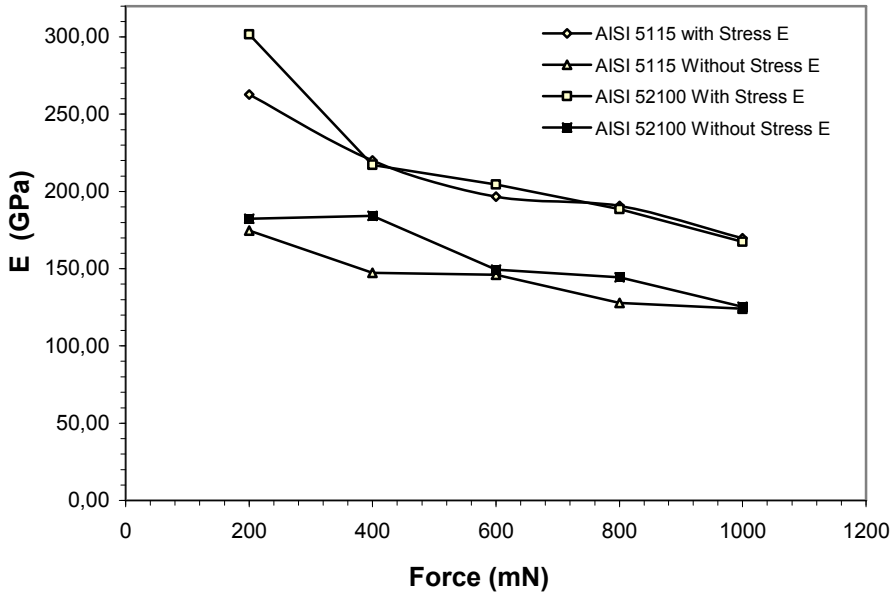


**Figure 6:** Young's modulus variations of AISI 5115 and AISI 52100 with and without stress

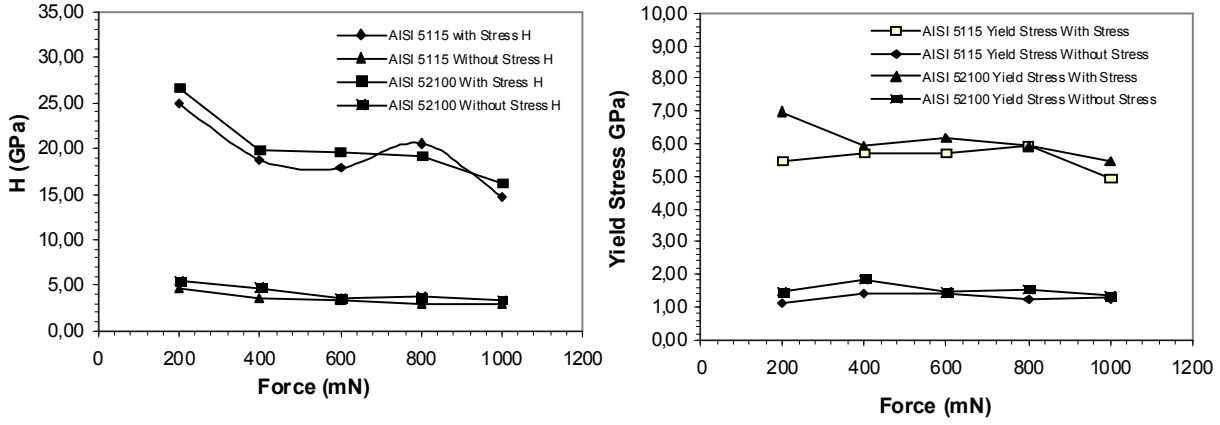


**a)** **b**

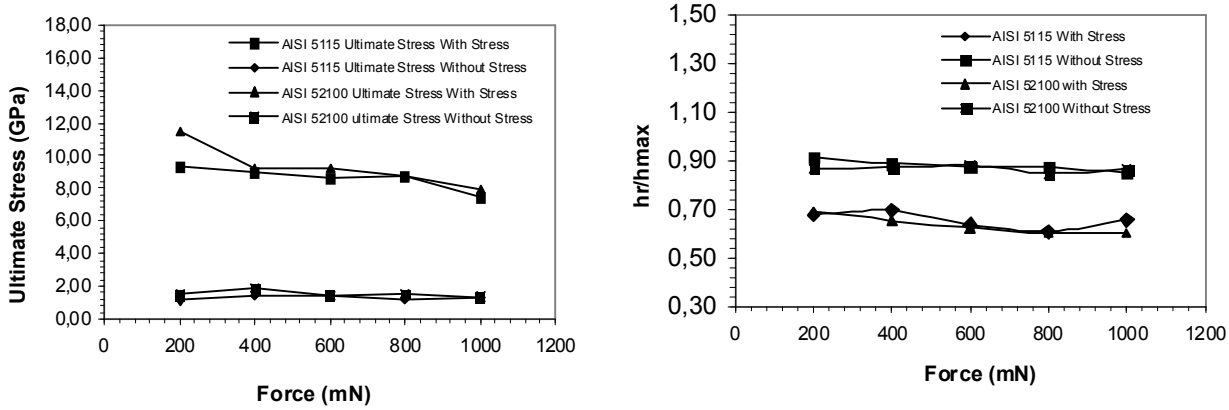

**c)** **d)**

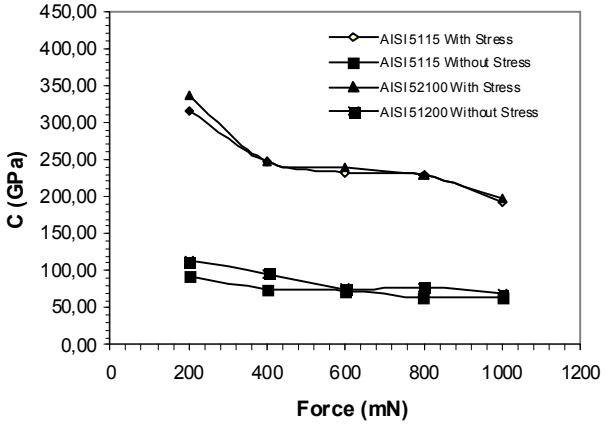


**e)**

**Figure 7: a)** Hardness **b)** Yield Stress **c)** Ultimate Stress **d)** $h_r/h_{max}$ and **e)** C –Force curves of AISI 5115 and 52100 quality steel (with and without stress)

Hardness study of samples is shown in Figure 7 a). When the applied loads increased from 200 to 1000 mN, hardness values of AISI 5115 and 52100 quality steel were decreased from 5,40 to 3,64 GPa and 4,38 to 3,38 GPa, respectively. After heat treatment regime and compressive residual stress (reduction of contact area), hardness of samples increased as 26,60 to 14,69 GPa and 24,92 and 16,09 GPa for AISI 5115 and 52100 quality steels under same applied loads.

Yield and ultimate stress of samples were determined by analyzing the indentation load–depth data according to the step by step procedure (Suresh & Giannakopoulos, 1998). This calculation procedure was applied for both AISI 5115 and 52100 quality steels and their heat treated samples. Yield and ultimate stress values differences between virgin and heat treated samples were given in Figure 7 b) and c). Each result influenced from applied loads and indentation size effect active in this model.

$h_r/h_{max}$ and C values of samples is indicated the elastic properties. C is active in loading part of indentation curve as $P=Ch^2$. As shown in Figure 5 and Figure 7 e), C values of heat treated samples increased depending applied loads.

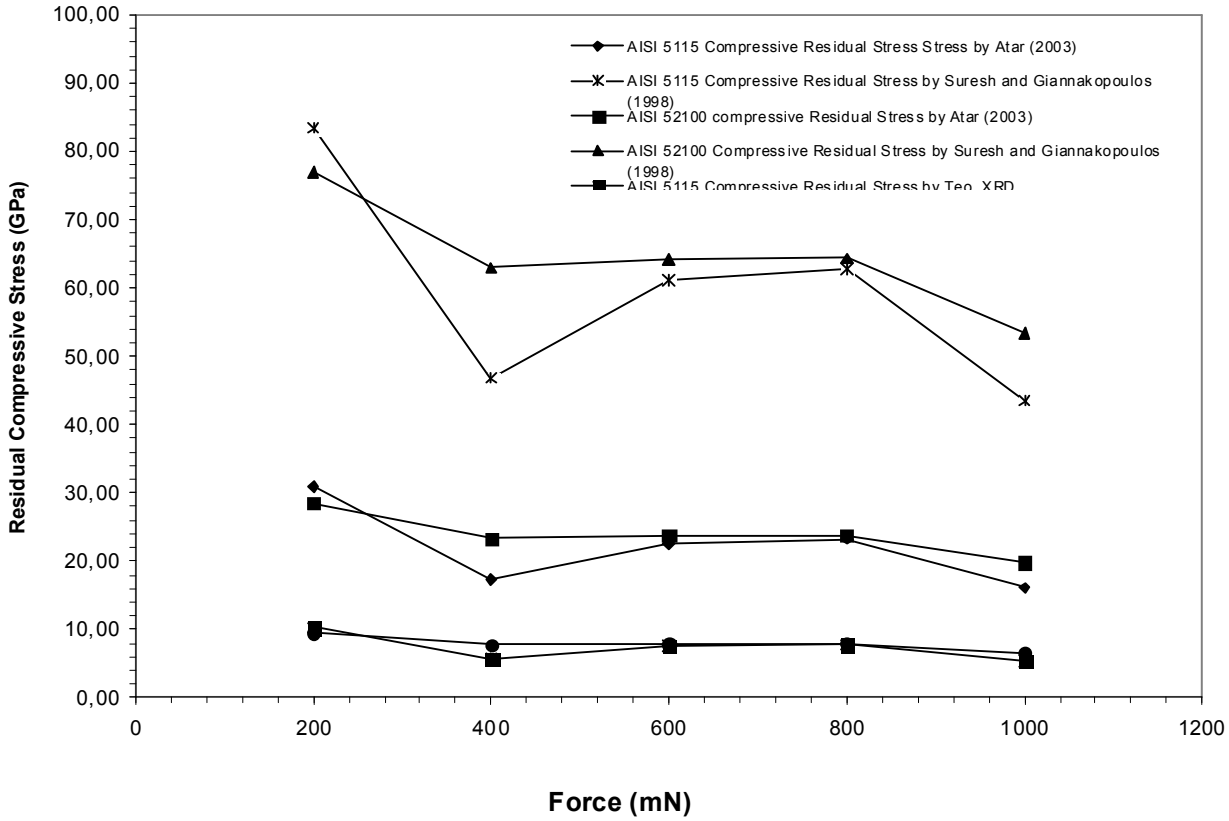


**Figure 8:** Residual Compressive Stress variations (for two different theories) of AISI 5115 and 52100 quality steels under different applied loads

The residual stress values of AISI 5115 and 52100 quality steels determined by the instrumented indentation method were found and represented in Figure 8. Atar et al. (2003) and Suresh & Giannakopoulos (1998) methods were applied to indented samples and calculation results showed that differences of contact area calculation is directly effect the residual stress results.

## References


Asi, O. & Asi, D. (2003). An investigation of residual stresses developed in carburized SAE 8620 steel. *Gazi University Journal of Science* 16, 725-732.

Atar, E., Sarıoğlu, C. et al. (2003). Residual stress estimation of ceramic thin films by X-ray diffraction and indentation techniques. *Scripta Materialia* 48, 1331-1336

Chen, X., Yann, J., Anette, M.K. (2006). On the determination of residual stress and mechanical properties by indentation. *Materials Science and Engineering: A* 46, 139-149.

Dilmeç, M., Yiğit, O., Halkacı, H.E.(2008). Measurement of residual stresses with layer removal method and comparison with other methods. *Mühendis ve Makine* 49, 20-27.

Dub, S., Novikov, N., Milman, Y. (2002). The transition from elastic to plastic behaviour in an Al-Cu-Fe quasicrystal studied by cyclic nanoindentation. *Philosophical Magazine A* 82, 2161–2172.

Karataş, Ç., Fetullayev, E., Kafkas, F. (2001). The research into the residual stresses on the root's teeth of a gear wheel made of AISI 5115 steel. *Journal of Faculty Engineering Architecture Gazi University* 16, 9-18.

Oliver, W.C. & Pharr, G.M. (1992). An improved technique for determining hardness and elastic-modulus using load and displacement sensing indentation experiments. *Journal of Materials Research* 7, 1564-1583.

Nishibori, M. & Kinoshita, K. (1978). Ultra-microhardness of vacuum-deposited films I: Ultra-microhardness tester. *Thin Solid Films* 48, 325-331.

Reibold, M., Belger, A. et al. (2005). The impact of nanoindentation at room temperature upon the real structure of decagonal AlCoNi quasicrystals. *Physica Status Solidi A-Applications and Materials Science* 202, 2267–2276.

Sahin, S., Toparli, M. et al. (2003). Modelled and measured residual stress in a biomaterial joint. *Journal of Materials Processing Technology* 132, 235-241.

Stickels, C.A. & Janotik, A.M. (1980). Controlling residual stress in 52100 bearing stress by heat treatment. *Metallurgical and Materials Transactions A* 11, 467-473.

Suresh, S. & Giannakopoulos A.E. (1998). A new method for estimating residual stresses by instrumented sharp indentation. *Acta Materialia* 46, 5755-5767.

Turski, M. & Edwards, L. (2009). Residual stress measurement of a 316l stainless steel bead-on-plate specimen utilising the contour method. *International Journal of Pressure Vessels and Piping* 86, 126-131

Uzun, O., Kölemen, U. et al. (2005). Modulus and hardness evaluation of polycrystalline superconductors by dynamic microindentation technique. *Journal of the European Ceramic Society* 25, 969-967.